



Automatic Extraction of a Piecewise Symmetry Surface of a 3D Mesh: Application to Scoliosis

Marion Morand^{1,2}(✉), Olivier Comas², Gérard Subsol¹, and Christophe Fiorio¹

¹ Research-Team ICAR, LIRMM, University of Montpellier/CNRS, Montpellier, France

{gerard.subsol,christophe.fiorio}@lirmm.fr

² DMS Imaging, Nîmes, France

{mmorand,ocomas}@dms-imaging.com

Abstract. Symmetry analysis of the surface of anatomical structures offers good promise for diagnosis, follow-up and therapy planning of pathologies causing abnormal deformities. This paper addresses the problem of detecting and modelling symmetry of bilateral structures, even in cases where the transformation between the two lateral parts is not a simple planar reflection but a symmetry with respect to a curved symmetry surface. We describe a new method to compute a piecewise curved symmetry surface for 3D objects. The algorithm is based on the computation of a 3D symmetry line, which defines strips by orthogonal slicing. A local symmetry plane is computed for each strip by an ICP-like method. The set of all local symmetry planes forms a piecewise symmetry surface. The method is first validated on parametric objects. Then, we show its potential as a non-invasive technique for the study of patients affected by scoliosis. Finally, our approach is generic enough that it could be extended to other medical applications such as facial dysplasia.

Keywords: Symmetry analysis · Curved reflection · Scoliosis

1 Introduction

Reflection is one of the main characteristics of many human anatomical structures. Its loss is often linked to pathologies causing abnormal deformities. Analysis of the 3D symmetry of the anatomical structure surface gives very useful information for diagnosis, follow-up or therapy planning. With the development of 3D medical imaging, quantifying automatically the symmetry in 3D data of anatomical structures (either as 3D image or 3D mesh) has become an important research topic in medicine, especially for brain [17], face [7] or back pathologies [9]. For example, some recent work [17] on the brain proposed an algorithm to extract a 3D symmetry surface, which results in a better left/right hemisphere segmentation. Moreover, the deviation of this symmetry surface with respect to the anatomical sagittal plane allows one to characterise brain torque [11].

© Springer Nature Switzerland AG 2018

M. Reuter et al. (Eds.): ShapeMI 2018, LNCS 11167, pp. 147–159, 2018.

https://doi.org/10.1007/978-3-030-04747-4_14

Nevertheless, most of the work dealing with algorithms to detect automatically 3D symmetry in anatomical structures focuses on planar symmetry [15]. Symmetry is then quantified by finding a symmetry plane Π , aligning the original structure with its corresponding reflection with respect to this plane and by analysing point-to-point distances [10]. For a straight bilateral structure, there exists a unique reflected point y that corresponds to a point x with respect to Π and conversely. However, it is well-known that most of bilateral anatomical structures do not present a planar symmetry but a “curved” symmetry [13]. In this case, we may not have a unique correspondence between x and y but several reflected points y_i for a unique original point x (see Fig. 1).

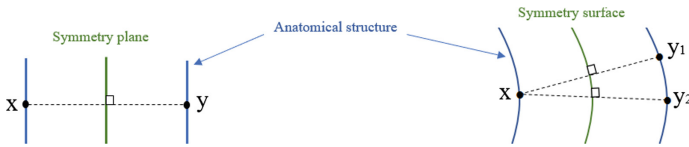


Fig. 1. Differences between a planar and a curved symmetry

Related Work. Methods to compute curved symmetry surfaces can be separated into three groups.

The first group of methods is based on 2D slicing. Lee *et al.* [12] cut the 3D structure along parallel planes and get a set of 2D slices. They then propose an algorithm to obtain a 2D curved glide-reflection symmetry for each slice. By interpolating all the 2D symmetry curves, they obtain a parametric 3D symmetry surface. However, their method depends heavily on the chosen orientation for the 2D slicing procedure.

The second group is based on a refinement of a global symmetry plane. Sato *et al.* [16] use the Hough transform to estimate an initial symmetry plane. Two refinement processes to obtain a symmetry surface are then proposed. The first one uses a quadratic fitting function instead of a plane. The second process consists in applying the planar symmetry detection method only to the contour points within a local window and extracting the curved symmetry by linking local planar symmetries detected at each point along the occluding contour. In his Ph.D. thesis, Combès [3] computes an initial symmetry plane by an ICP-based method and divides the 3D mesh orthogonally to this plane. For each submesh, a new symmetry plane is estimated and the surface of symmetry is globally parametrised with a Leclerc function. It is then assumed that the curved symmetry can be seen locally as a planar symmetry. However, the results of this group of methods are limited to anatomical structures which are not too curved due to the global smoothness of the fitting functions.

A third group can be defined by the approaches that are specific to brain applications. They are based on 3D MR images of the brain and use the variation of intensities of the cerebral structures. For example, Kuijf *et al.* [11] segment

the brain in the MR image and detect automatically the interhemispheric fissure that gives an initial symmetry plane. Then, control points are defined to deform this initial symmetry plane into an optimised surface, modelled by a bicubic spline. After the approximation of a symmetry plane of the brain, Davarpanah *et al.* [5] propose a refinement process that is applied on 2D slices of the 3D MR images based on fractal dimension and specific intensity values of the cerebral structures. A symmetry surface is eventually constructed as a stack of resulting curves in different slices. Stegman *et al.* [17] suggest to compute symmetry pixels in 2D slices of the 3D MR brain image maximising a local symmetry measure based on a correlation coefficient and the image intensity at the slice centre voxel. All these methods cannot be directly generalised to other anatomical structures, especially if the latter are given as 3D meshes.

Contributions. Due to the 2D character of the first class of methods and the specific application of the third class, we choose to focus on the second class and propose to generalise their application to large bending.

In this paper, we introduce a new method for automatically assessing the curved reflection of a 3D mesh by extraction of a piecewise symmetry surface. We present this algorithm in detail in Sect. 2: a set of local symmetry planes is computed and forms a piecewise symmetry surface. In Sect. 3, we assess our approach on parametrical 3D meshes. In Sect. 4, we study its application to 3D meshes of the back of patients affected by scoliosis.

2 Piecewise Symmetry Surface Extraction

Our method is designed to automatically detect a piecewise symmetry surface of a 3D mesh even in the case of a very curved structure. In practice, we choose to decompose the 3D mesh into a set of strips S_i which are defined orthogonally to a free-form 3D curve L which we call “symmetry line” and then compute their planes of symmetry Π_i . The method is iterative and begins with an initial symmetry line and strips. At each step n , we get a new set of Π_i^n . At the end of the iterative process, when the symmetry line is stable, we obtain an optimised set of local symmetry planes that we fuse to form the piecewise symmetry surface of the 3D mesh. The overview of the iterative method is illustrated Fig. 2 and we describe each step in the following.

2.1 Determination of the Initial Symmetry Line and Strips

To initialise the symmetry line and the strips, we decompose roughly the 3D mesh into submeshes that we call regions where the symmetry is consistent. For this, the user manually defines two points on the 3D mesh that describe a straight line. Between this couple of points and perpendicularly to the direction of the line, we define N_R regions delimited by $(N_R + 1)$ equidistant and parallel planes. N_R is defined by the user.

The Principal Component Analysis (PCA) method is applied to every sub-mesh to compute their principal axis for a coarse estimate of the direction of the

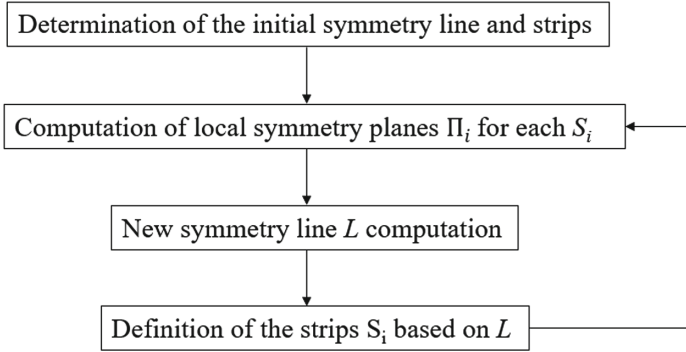


Fig. 2. Piecewise symmetry extraction method

regions. We then subdivide each region orthogonally to its axis into N_S equidistant surface strips S_i . This step is illustrated Fig. 3. In fact, the N_R axes define the initial symmetry line.

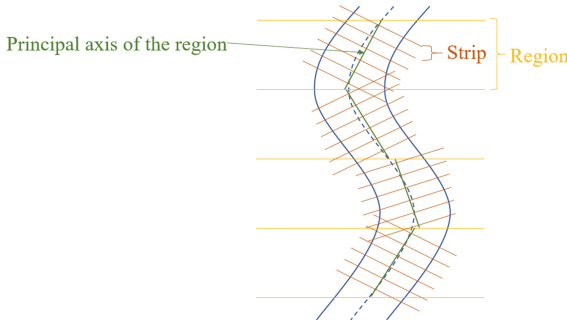


Fig. 3. 2D illustration of the computation of the initial symmetry line and strips

In practice, for general objects, the two seed points are chosen at the extremities of the structure and belonging to the symmetry surface.

2.2 Computation of Local Symmetry Planes

Initialisation. If a surface is perfectly symmetrical, it is well-known that its symmetry plane is orthogonal to a PCA axis [18]. So PCA is used to initialise the symmetry plane Π_i^0 for each strip S_i . We roughly define the direction of the symmetry and the PCA axis that has the closest orientation is selected to act as the normal unit vector \mathbf{u}_i^0 of Π_i^0 . We assume that Π_i^0 goes through the centroid of S_i which defines the distance d_i^0 to the origin. The couple (\mathbf{u}_i^0, d_i^0) gives an initial symmetry plane Π_i^0 for each strip S_i .

Optimisation. For each strip S_i , we launch the Iterative Closest Point (ICP)-like algorithm described in [4]. This method directly computes the parameters of the optimal symmetry plane for bilateral objects presenting a perfect or imperfect reflection symmetry. To make the method more robust, we integrate the TrimmedICP (trICP) algorithm proposed by Chetverikov *et al.* [2]. While the standard ICP algorithm assumes that all data points can be paired, trICP rejects outliers points. The optimisation of the symmetry plane localisation follows an iterative scheme. At iteration n of the algorithm, we have the 3 following steps:

- (1) The points of the strip S_i are reflected with respect to the current estimated symmetry plane Π_i^n . Using the k-d tree method, each point \mathbf{x}_k of S_i is paired with the closest reflected point of S_i . From the set of registered point couples $(\mathbf{x}_k; \mathbf{y}_k^n)$ obtained, the individual squared distances are computed and sorted in increasing order. We only select the first $q_i N_i$ couples of points, with q_i the overlap rate from the trICP and N_i the number of points included in the strip S_i . The optimal value of q_i is searched in a range of $[0.4; 1.0]$ by minimising the Mean Squared Error of distance $(\mathbf{x}_k, \mathbf{y}_k^n)$ while trying to use as many points as possible [2]. Notice that $(\mathbf{x}_k, \mathbf{y}_k^n)$ is different at each step as it depends on Π_i^n .
- (2) The parameters $(\mathbf{u}_i^{n+1}, d_i^{n+1})$ of the new estimation of the symmetry plane of S_i are computed by the two following formulas given in [4]:
 - \mathbf{u}_i^{n+1} is collinear with the eigenvector corresponding to the smallest eigenvalue of the 3×3 matrix U_{n+1} defined as:

$$U_{n+1} = \sum_{(\mathbf{x}_k; \mathbf{y}_k^n)} (\mathbf{x}_k - \mathbf{g}_1 + \mathbf{y}_k^n - \mathbf{g}_2)(\mathbf{x}_k - \mathbf{g}_1 + \mathbf{y}_k^n - \mathbf{g}_2)^T - (\mathbf{x}_k - \mathbf{y}_k^n)(\mathbf{x}_k - \mathbf{y}_k^n)^T$$

$$\text{with } \mathbf{g}_1 = \frac{1}{N} \sum \mathbf{x}_k \text{ and } \mathbf{g}_2 = \frac{1}{N} \sum \mathbf{y}_k^n.$$

$$- d_i^{n+1} = \frac{1}{2}(\mathbf{g}_1 + \mathbf{g}_2)^T \mathbf{u}_i^{n+1}$$

- (3) Go back to step 1 if the mean distance between $(\mathbf{x}_k, \mathbf{y}_k^n)$ has changed between the iterations and if a maximal number of iterations has not been reached.

Finally, we obtained a local symmetry plane Π_i for each strip S_i and therefore a set of local symmetry planes which forms the piecewise symmetry surface.

2.3 New Symmetry Line Computation

For each Π_i , we note $\mathbf{P}_i^{\text{inf}}$ and $\mathbf{P}_i^{\text{sup}}$ the 2 points that are defined at the intersection between the surface, Π_i and respectively the inferior and superior plane of the strip. We compute the $(N_S + 1)$ symmetry points $\mathbf{P}_i^{\text{sym}}$ as the middle between $\mathbf{P}_i^{\text{sup}}$ and $\mathbf{P}_{i+1}^{\text{inf}}$ (see Fig. 4). The new symmetry line L is formed by the interpolation of the set of symmetry points $\mathbf{P}_i^{\text{sym}}$ by a third order parametric spline curve.

2.4 Definition of the Strips Based on the Symmetry Line

This symmetry line L acts as a base for creating new adaptive strips S_i^a (see Fig. 5). Each new adaptive strip S_i^a is defined as the intersection between the object surface and two planes:

- The superior plane of the strip is characterised by the vector defined by \mathbf{P}_{i+1}^{sym} and \mathbf{P}_{i+2}^{sym} and passing through \mathbf{P}_{i+1}^{sym} .
- The inferior plane of the strip is characterised by the vector defined by \mathbf{P}_i^{sym} and \mathbf{P}_{i-1}^{sym} and passing through \mathbf{P}_i^{sym} .

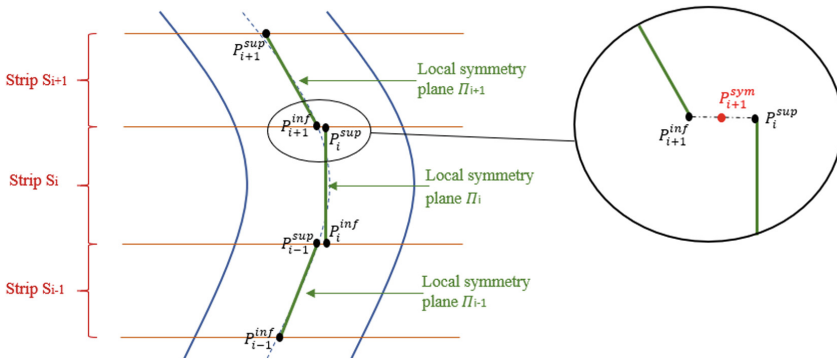


Fig. 4. 2D illustration of the computation of the symmetry points

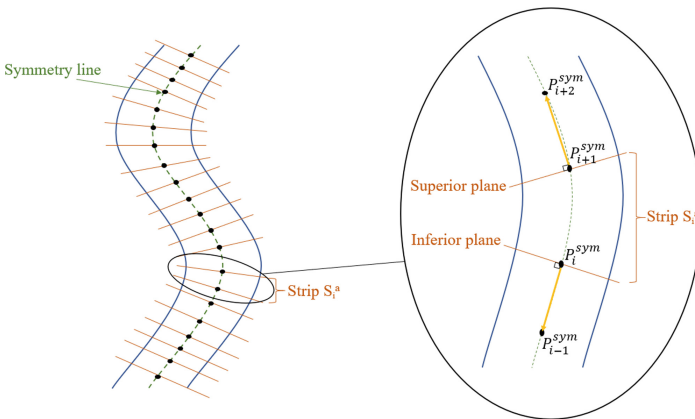


Fig. 5. 2D illustration of the strip refinement

3 Validation on Parametrical 3D Meshes

3.1 Method





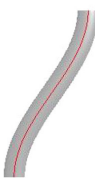



To validate our method on objects presenting curved reflection, we generate mathematically different swept 3D meshes which are curved and we assess the method accuracy with respect to bending. We define a half-ellipse in the plane (Oxy) centered in $(0, 0, 0)$, with a semi-major axis of 20 mm along Ox and a semi-minor axis of 10 mm along Oy . The symmetry point of this half-ellipse is then located at $(0, 5.0, 0)$. We extrude this curve along a 3D parametric curve involving cosine and sine. Each model is sampled into a 3D mesh made of 75 000 vertices. The set of meshes is shown in the Table 1. The extrusion of the symmetry points of the half-ellipse gives the symmetry line. For a height z , the theoretical local symmetry plane is given by the binormal of the Frenet-Serret frame along this symmetry line.

We can then compare our piecewise symmetry surface to this theoretical plane both in localisation and orientation. For the localisation we compute the depth and lateral Root Mean Square Deviations, defined as the quadratic mean of the distances projected along an axis: Oy for RMSD_{depth} and Ox for RMSD_{lat} . We assess the orientation of each local symmetry plane by calculating the angle θ defined as $\theta = \arccos(\mathbf{n} \cdot \mathbf{u})$, where \mathbf{n} is the normal unit vector of the theoretical symmetry plane and \mathbf{u} is the normal unit vector of the symmetry plane obtained by our method.

3.2 Results

Our method was implemented in Matlab (R2015a). We have chosen 4 regions ($N_R = 4$) and 5 strips have been created in each of them ($N_s = 5$). The number of iterations is arbitrarily fixed at 100 for each strip. Table 1 shows the comparison of our piecewise symmetry surface (in red) with the theoretical one.

Table 1. Evaluation of the proposed method on geometrical swept models

Model	1	2	3	4	5	6	7
							
RMSD_{lat} (mm)	0.16	0.50	0.64	0.80	0.62	1.10	1.75
RMSD_{depth} (mm)	0.00	0.01	0.02	0.02	0.01	0.03	0.09
Mean value θ ($^\circ$)	0.5	1.3	1.9	2.2	1.8	2.8	4.0
Maximum value θ ($^\circ$)	2.1	2.37	4.5	5.9	3.9	6.4	11.1

The maximums for both the distance and the orientation θ are always observed at the apex section of the curve. This can be explained by the definition of the local symmetry plane. We assume that for a planar symmetry and by extension for small bending surface, we have $\mathbf{x}_k = \mathbf{S}_\Pi(\mathbf{y}_k^n)$ and $\mathbf{y}_k^n = \mathbf{S}_\Pi(\mathbf{x}_k)$. However, for large bending $\mathbf{y}_k^n = \mathbf{S}_\Pi(\mathbf{x}_k)$ is not guaranteed. This is why the orientation of our plane does not perfectly match the orientation of the Frenet-Serret frame, which is only an approximate solution along the translated 3D curve used as trajectory during the mesh generation. We observe that one iteration of the refinement is enough to obtain stable symmetry lines and good results, but it may be necessary to carry out additional iterations for more complex structures.

Comparing to other existing methods, our method promises good results. The method proposed by Sato *et al.* [16] seems to fail for surfaces with a single bending which is smaller than ours. In the same way, the methods proposed by Combès [3] and Lee *et al.* [12] are limited for detecting symmetry of structures with large or multiple curvatures, due to their initialisations. In particular, the initial slicing process of the 3D mesh proposed by [12] is only parallel and so will negatively affect the results in case of curved structures.

4 Application to Scoliosis

Scoliosis is characterised by a lateral deviation of the spine, associated to a local axial rotation of vertebrae in the horizontal plane. This 3D spinal deformity may lead to severe impairment of the outer appearance of the back surface. To limit hazardous X-ray examinations prescribed during the treatment, there is a growing interest for non-invasive methods based on 3D measurements of the back mesh [1, 9].

The aim of these methods is to find 3D parameters that yield better quantification of the back deformation. In particular, one of the interesting parameters to assess scoliosis is the left/right asymmetry in order to determine the number, direction and location of deformed parts for classifying the scoliosis [1]. We apply our method to the 3D meshes of the backs of patients affected by scoliosis with the following parameters:

- The initial direction of the subdivision of the back into regions is computed from the straight line defined by the prominent vertebra and the middle of the posterior superior iliac spine. In order to fully automate the method, the detection of these anatomical landmarks may be based only on the surface curvature as proposed in [8].
- We used 3 regions and 6 strips per regions to represent the 18 vertebrae localised between the two seed points. An adaptation of the height of each strip to the height of each vertebra is statistically computed from the height of the spine.

The result on one example of a scoliotic patient can be seen in Fig. 6.

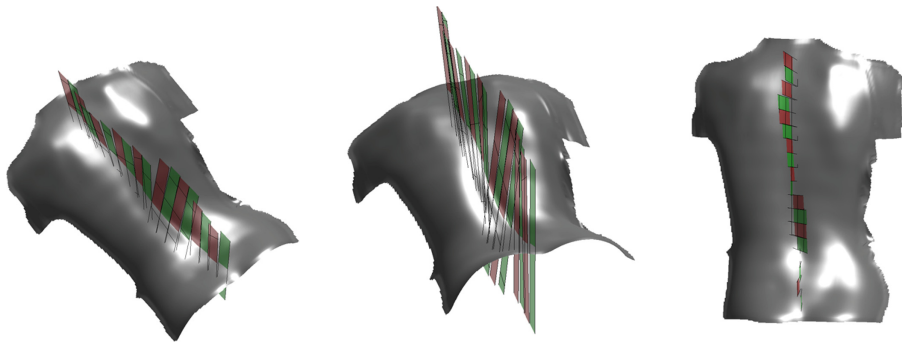


Fig. 6. 3D piecewise symmetry surface of the back of a scoliotic patient. Notice how the orientations of the local planes (in green and red) follow the back deformations. (Color figure online)

4.1 Symmetry Line of the Back Mesh

The lateral deviation and the anteroposterior curvature are measured with respect to the spinal midline, which is the line that passes over the centre point of the vertebral bodies. The midline can be estimated by the symmetry line of the back shape [9]. We have already showed the potential of a simpler version of our method to compute the symmetry line for 3D objects [14]. The comparison between the line manually determined by landmarks placed by clinician and this symmetry line assesses the mean error deviation to 5.8 mm, the $RMSD_{lat}$ to 4.82 mm and the $RMSD_{depth}$ to 0.69 mm. These indicators remain constant with the variations of the disease severity and patient morphology. These results demonstrate that the method is consistent with the reference method and robust with respect to the disease severity and the patient morphology.

4.2 Vertebral Rotation

We propose to use our new method to evaluate the local back surface rotation that can be correlated to the axial rotations of vertebrae [9]. 51 scoliotic patients were acquired with the BIOMODTM system¹. This device provides bi-planar radiographic 3D reconstructions of the spines coupled with optical acquisitions of back surfaces. They are both expressed in a patient-specific reference system. For each vertebra, we have the 3D coordinates of the spinous process, noted S , and the centre of the vertebra C . We compute the direction SC and we recover its projection in the horizontal plane. In the same way, we compute the horizontal component of the direction provided by the local symmetry plane corresponding to the same vertebra. We compute α the angle between these two directions, as illustrated Figs. 7 and 8, for each vertebra for every patient. On the set of

¹ Acquisition device developed by AXS Medical (DMS Imaging): <http://www.dms.com/biomod-3s/>.

the 51 patients, we get: $\alpha = 3.81^\circ \pm 2.93^\circ$. This preliminary result seems to be promising, considering those presented in [8].

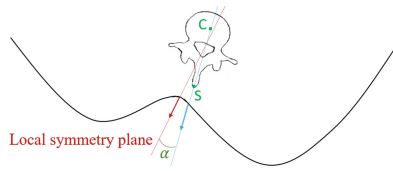


Fig. 7. Comparison between the orientation of the local symmetry plane and the actual vertebral rotation

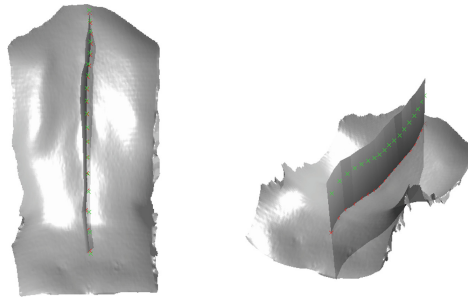


Fig. 8. Example of a piecewise symmetry surface on the back of a scoliotic patient. Note that red crosses correspond to spinous processes on the back surface and green crosses to the centre of vertebrae. (Color figure online)

4.3 Adaptation to the Lateral Bending Posture

Patients are often examined in lateral bending as this position is optimal to evaluate the spine flexibility for surgery planning. However most of the proposed methods to analyse this pathology fail for asymmetric postures [6]. We apply our method on a patient in bending posture (Fig. 9). Notice how the spine curve is well emphasised by the piecewise symmetry surface.

5 Future Work

We have described a method for computing out a piecewise symmetry surface on 3D meshes. Future work will focus on interpolating the piecewise surface to obtain a continuous curved symmetry surface. To provide reproducible and objective results, a fully automatic calculation of the method parameters (N_R

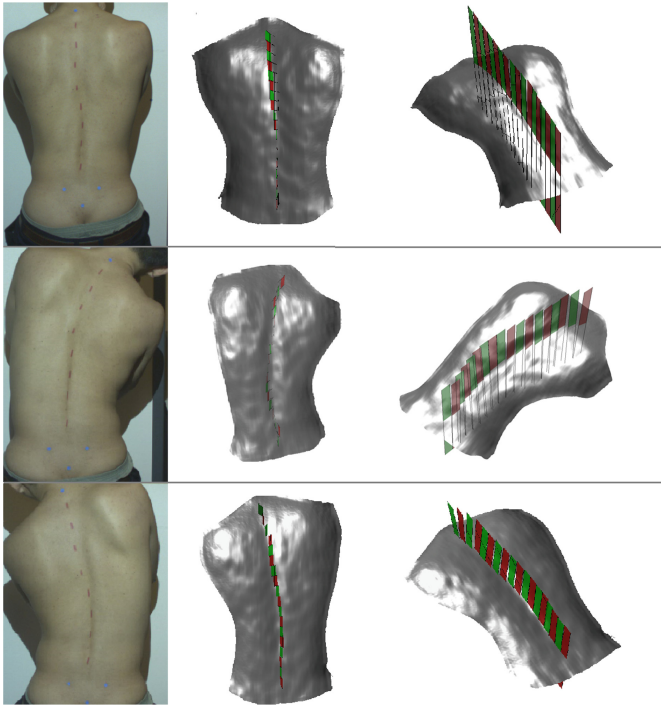


Fig. 9. Piecewise symmetry surface on the 3D meshes of the back of a patient in bending ($\sim 180\,000$ vertices and $\sim 360\,000$ faces).

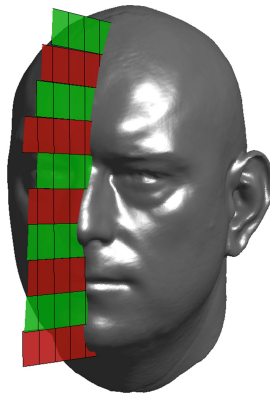


Fig. 10. Computation of a piece wise symmetry surface of a 3D face mesh ($\sim 41\,000$ vertices and $\sim 81\,500$ faces)

and N_s in particular) based only on the 3D geometry will be proposed. On the clinical side, we also plan to use our local symmetry planes for classification of scoliosis [1]. Moreover, our approach could be extended to other medical applications such as facial dysplasia (see for example Fig. 10).

Acknowledgements. This work was supported by a CIFRE grant (French National Association of Research and Technology) for the doctoral work of Marion Morand.

References

1. Aroeira, R.M.C., de Las Casas, E.B., Pertence, A.E.M., Greco, M., Tavares, J.M.R.: Non-invasive methods of computer vision in the posture evaluation of adolescent idiopathic scoliosis. *J. Bodyw. Mov. Ther.* **20**(4), 832–843 (2016)
2. Chetverikov, D., Svirko, D., Stepanov, D., Krsek, P.: The trimmed iterative closest point algorithm. In: 16th International Conference on Pattern Recognition, vol. 3, pp. 545–548 (2002)
3. Combès, B.: Efficient computational tools for the statistical analysis of shape and asymmetry of 3D point sets. Ph.D. thesis. Signal and Image Processing, University of Rennes 1 (2010)
4. Combès, B., Hennessy, R., Waddington, J., Roberts, N., Prima, S.: Automatic symmetry plane estimation of bilateral objects in point clouds. In: 26th IEEE Conference on Computer Vision and Pattern Recognition, Anchorage, US (2008)
5. Davarpanah, S.H.: Brain mid-sagittal surface extraction based on fractal analysis. *Neural Comput. Appl.* **30**(1), 153–162 (2018)
6. Di Angelo, L., Di Stefano, P., Spezzaneve, A.: Symmetry line detection for non-erected postures. *Int. J. Interact. Des. Manuf.* **7**(4), 271–276 (2013)
7. Di Angelo, L., Di Stefano, P.: Bilateral symmetry estimation of human face. *Int. J. Interact. Des. Manuf.* **7**(4), 217–225 (2013)
8. Drerup, B., Hierholzer, E.: Back shape measurement using video rasterstereography and three-dimensional reconstruction of spinal shape. *Clin. Biomech.* **9**(1), 28–36 (1994)
9. Drerup, B.: Rasterstereographic measurement of scoliotic deformity. *Scoliosis* **9**(1), 22 (2014)
10. Krajčiček, V., Dupej, J., Velemínská, J., Pelikán, J.: Morphometric analysis of mesh asymmetry. *J. WSCG* **20**(1), 65–72 (2012)
11. Kuijf, H.J., Veluw, S.J.V., Geerlings, M.I., Viergever, M.A., Jan, G., Koen, B.: Automatic extraction of the midsagittal surface from brain MR images using the Kullback–Leibler measure. *Neuroinformatics* **12** (2013)
12. Lee, S., Liu, Y.: Curved glide-reflection symmetry detection. *IEEE Trans. Pattern Anal. Mach. Intell.* **34**(2), 266–278 (2012)
13. Lee, T.S.H., Fidler, S., Dickinson, S.: Detecting curved symmetric parts using a deformable disc model. In: IEEE International Conference on Computer Vision, Sydney, Australia, pp. 1753–1760 (2013)
14. Morand, M., Comas, O., Fiorio, C., Subsol, G.: Automatic extraction of the 3D symmetry line of back surface: application on scoliotic adolescents. In: 40th International IEEE Conference on Engineering in Medicine and Biology Society, EMBS, Honolulu, US (2018)
15. Quan, L., Zhang, Y., Tang, K.: Curved reflection symmetric axes on free-form surfaces and their extraction. *IEEE Trans. Autom. Sci. Eng.* **15**(1), 111–126 (2018)

16. Sato, Y., Tamura, S.: Detecting planar and curved symmetries of 3D shapes from a range image. *Comput. Vis. Image Underst.* **64**(1), 175–187 (1996)
17. Stegmann, M.B., Skoglund, K., Ryberg, C., Plads, R.P., Lyngby, D.K.: Mid-sagittal plane and mid-sagittal surface optimization in brain MRI using a local symmetry measure. In: *Medical Imaging 2005: Image Processing*, vol. 5747, pp. 568–579 (2005)
18. Sun, C., Sherrah, J.: 3D symmetry detection using the extended Gaussian image. *IEEE Trans. Pattern Anal. Mach. Intell.* **19**(2), 164–169 (1997)